European Journal of Pharmaceutical Sciences 168 (2022) 106056

Contents lists available at ScienceDirect

European Journal of Pharmaceutical Sciences

journal homepage: www.elsevier.com/locate/ejps

Application of *in vitro* PAMPA technique and *in silico* computational methods for blood-brain barrier permeability prediction of novel CNS drug candidates

Milica Radan, Teodora Djikic *, Darija Obradovic, Katarina Nikolic **

University of Belgrade - Faculty of Pharmacy, Department of Pharmaceutical, Chemistry, Vojvode Stepe 450, 11000 Belgrade, Serbia

ARTICLE INFO

Keywords:
hDAT
CNS drugs
PAMPA
QSPR
SMD
Blood-brain barrier permeability

ABSTRACT

Permeability assessment of small molecules through the blood-brain barrier (BBB) plays a significant role in the development of effective central nervous system (CNS) drug candidates. Since *in vivo* methods for BBB permeability estimation require a lot of time and resources, *in silico* and *in vitro* approaches are becoming increasingly popular nowadays for faster and more economical predictions in early phases of drug discovery. In this work, through application of *in vitro* parallel artificial membrane permeability assay (PAMPA-BBB) and *in silico* computational methods we aimed to examine the passive permeability of eighteen compounds, which affect serotonin and dopamine levels in the CNS. The data set was consisted of novel six human dopamine transporter (hDAT) substrates that were previously identified as the most promising lead compounds for further optimisation to achieve neuroprotective effect, twelve approved CNS drugs, and their related compounds. Firstly, PAMPA methods was used to experimentally determine effective BBB permeability (P_e) for all studied compounds and obtained results were further submitted for quantitative structure permeability relationship (QSPR) analysis. QSPR models were built by using three different statistical methods: stepwise multiple linear regression (MLR), partial least square (PLS), and support-vector machine (SVM), while their predictive capability was tested through internal and external validation. Obtained statistical parameters (MLR- R^2_{pred}=-0.10; PLS- R^2_{pred}=0.64, r^2_m=0.69, r'^2_m=0.44; SVM- R^2_{pred}=0.57, r^2_m=0.72, r'^2_m=0.55) indicated that the SVM model is superior over others. The most important molecular descriptors (H_0p and SolvEMt_3D) were identified and used to propose structural modifications of the examined compounds in order to improve their BBB permeability. Moreover, steered molecular dynamics (SMD) simulation was employed to comprehensively investigate the permeability pathway of compounds through a lipid bilayer. Taken together, the created QSPR model could be used as a reliable and fast pre-screening tool for BBB permeability prediction of structurally related CNS compounds, while performed MD simulations provide a good foundation for future *in silico* examination.

1. Introduction

Discovery of central nervous system (CNS) drugs that can successfully penetrate through blood-brain barrier (BBB) and reach desired therapeutic target is one of the most challenging tasks. Many CNS drug candidates failed to reach the market due to lack of the ability to cross the BBB. Therefore, getting early information about the compounds BBB permeability is of great importance in all drug discovery processes (Kerns and Di, 2002; Nielsen et al., 2011).

BBB is highly selective barrier which separates the brain from the rest of the body. It is made of specialized tight junctions between brain endothelial cells. For this reason, BBB is a major obstacle in the discovery of new drugs for efficient treatment of CNS-related diseases, since they are required to penetrate the barrier in order to reach their intended brain targets. Contrary, drugs with targets in peripheral tissues also need to be investigated for their BBB permeability to avoid CNS side effects (Abbott et al., 2006; Nielsen et al., 2011). The two main mechanisms are available for a molecule to pass through BBB: passive and

* Corresponding author at: Research Associate, Department of Pharmaceutical Chemistry, Faculty of Pharmacy, University of Belgrade, Vojvode Stepe 450, 11000 Belgrade, Serbia.

** Co-corresponding author at: Associate Professor, Department of Pharmaceutical Chemistry, Faculty of Pharmacy, University of Belgrade, Vojvode Stepe 450, 11000 Belgrade, Serbia.

E-mail addresses: tdjikic@pharmacy.bg.ac.rs (T. Djikic), knikolic@pharmacy.bg.ac.rs (K. Nikolic).

https://doi.org/10.1016/j.ejps.2021.106056
Received 12 July 2021; Received in revised form 9 October 2021; Accepted 31 October 2021
Available online 2 November 2021

active. Passive diffusion is the most common way of passing through barrier, while active transport involves transport proteins (Clark, 2003).

Direct measurement of brain permeability is the most reliable method. However, this is a costly and time-consuming process. In order to avoid technically challenging processes for obtaining *in vivo* data, several *in vitro* and *in silico* methods are widely used in drug discovery (Abbott, 2004; Bicker et al., 2014; Nielsen et al., 2011). The most common methods for prediction of *in vitro* BBB permeability are parallel artificial membrane permeability assay (PAMPA-BBB) (Kansy et al., 1998), immobilized artificial membrane (IAM) chromatography (Yoon et al., 2006) and cell based assays (bovine brain microvessel endothelial cells (BBMEC), Madin-Darby canine kidney (MDCK) and Caco-2) (Garberg et al., 2005).

The PAMPA-BBB is high-throughput technique which is extensively used for predicting BBB permeability. Generally, it is based on the determination of the passive diffusion of molecules through artificial membrane that is made of polar brain lipids (PBL) in dodecane, which precisely mimic physicochemical microenvironment of the BBB (Avdeef, 2005; Di et al., 2003). A limitation of PAMPA is that neither active transport nor efflux by P-glycoprotein (P-gp) is modelled by the artificial membrane (Sugano, 2007; Sun et al., 2017). Despite this limitation, PAMPA method provides information about passive permeability through BBB, which is especially advantageous in early stages of drug discovery processes.

In addition, with continual increases in computer power, different *in silico* approaches have already been used for BBB-permeability prediction as viable alternatives for laborious experimental methods. Quantitative structure permeability relationship (QSPR) analysis plays an important role in elucidating the influence of different molecular properties on the penetration through BBB (Subramanian and Kitchen, 2003). In addition, molecular dynamics (MD) represents one of the most powerful *in silico* techniques to simulate the molecular process of diffusion at the atomic level (Carpenter et al., 2014; Thai et al., 2020).

Great efforts have been made in the field of treatment Parkinson's disease (PD) which is a neurodegenerative disorder characterized by the loss of dopaminergic neurons in the *substantia nigra* and *corpus striatum* (Dickson, 2012). Currently available drugs alleviate motor and non-motor symptoms but do not possess neuroprotective effect (Balestrino and Schapira, 2020). New drugs which target dopaminergic neurons through the dopamine transporter may provide a promising therapeutic strategy for establishing neuroprotective effect. Human dopamine transporter (hDAT) is expressed in dopaminergic neurons of the CNS. It is a main modulator of intrasynaptic dopamine levels and therefore provides normal neurological function (McHugh and Buckley, 2015). In our previous study, we have reported *in silico* approach for identification of promising hDAT substrates that were subsequently analysed *in vitro* (Djikic et al., 2019). Six compounds out of ten turned out to be substrates of hDAT (AO854/40003386, AM879/11741391, AG205/05879010, AO854/12910145, AP124/41027793, AP263/40017925) (Djikic et al., 2019). Besides, twelve other CNS drugs and their related compounds were included in this study. All selected compounds modulate activity of serotonergic or dopaminergic neurons in CNS, which are deeply involved in physiology and pathophysiology of various brain disorders. Substrates of hDAT, pramipexole and ropinirole are known to be effective in treatment of PD, while other studied CNS drugs are used as antidepressants or antipsychotics. Moreover, impurities of ziprasidone (Imp Z1 and Imp Z2) as well as aripiprazole impurity (Imp A1) were included in this data set. It is noteworthy that the Imp Z2 due to the presence of alkyl halide group possesses genotoxic potential which may affect drug's safety (Szekely et al., 2015).

The main aim of the current study was to determine BBB permeability of the above described eighteen structurally diverse compounds using PAMPA technique and to perform QSPR analysis in order to find out the most reliable and predictable *in silico* models for permeability prediction of related CNS compounds or their impurities. Additionally, work described herein is based on application of steered molecular dynamics (SMD) method as relatively fast pre-screening tool for BBB permeability prediction.

2. Materials and methods

2.1. Chemical and reagents

In this study analytical grade reagents: acetonitrile (J.T. Baker, Deventer, Netherlands), methanol (Merck, Darmstadt, Germany), acetic acid ≥ 99.8% (Sigma-Aldrich, St. Louis, MO, USA), ortho-phosphoric acid 85% (Merck, Darmstadt, Germany), ammonia solution 25% (Carlo Erba, Milano, Italy), and distilled water (TCA Purfication System, Neiderelbert, Germany) were used for the preparation of the mobile phase.

The porcine polar brain lipid (catalogue no. 141101C) was purchased from Avanti Polar Lipids, Inc. (Alabaster, AL). Also, dimethyl sulfoxide (DMSO) (Sigma-Aldrich, St. Louis, MO, USA), and dodecane (Sigma-Aldrich, St. Louis, MO, USA) were used throughout the study. The physiological buffer was prepared by using the sodium chloride (J. T. Baker, Deventer, Netherlands), sodium hydrogen phosphate, and potassium dihydrogen phosphate (Merck, Darmstadt, Germany).

The hDAT substrates were purchased from Specs (Zoetermeer, Netherlands). The following CNS standards: pramipexole dihydrochloride, citalopram hydrobromide, ropinirole hydrochloride, mirtazapine, risperidone, quetiapine fumarate, ziprasidone hydrochloride, olanzapine, Imp Z1 (3-(1-Piperazinyl)−1,2-benzisothiazole), Imp Z2 (6-chloro-5-(2-chloroethyl)−1,3-dihydro-2H-indol-2-one), Imp A1 (7,7′-(butylenedioxy)di-3,4-dihydroquinolin-2(1H)-one) and haloperidol were provided from Sigma-Aldrich (St. Louis, MO, USA).

All solutions prepared for HPLC analysis were passed through a 0.45 μm filter before use. The PAMPA 96-well plates (MultiScreen-HV, 0.45 lm, clear, non-sterile, cat. no. MAHVN4510) were purchased from the Millipore, Inc. (Bedford, MA).

2.2. Artificial membrane permeability assay

The eighteen structurally diverse neuroactive compounds (Fig. 1) were used for assessing the effective permeability at pH=7.40 with PAMPA-BBB model, as previously described in literature (Di et al., 2003; Vucicevic et al., 2015). The lipid membrane for PAMPA assay was prepared by dissolving 20 mg of porcine polar brain lipid (PBL) in 1 mL dodecane and 4 μL of prepared solution was used for coating the filter membrane. All examined compounds were dissolved in DMSO (5 mg/ml) and were subsequently diluted in physiological phosphate buffer (pH = 7.40) in order to obtain final concentration of 25 μg/ml.

The donor plates were filled with 300 μl of test solution, while the acceptor plate contains 300 μl of acceptor solution (physiological phosphate buffer). Then the acceptor plate was carefully placed on the top of the donor plate and created "sandwich" was left for 18 h incubation. After the incubation time the sandwich was disassembled and HPLC with UV detector was used for determination of the concentration of all examined compounds in each donor and acceptor wells, as well as in starting solutions. All compounds were analysed in triplicate and results are presented in mean values. Effective permeability of compounds was calculated using following Eqs. (1) and (2) (Avdeef, 2003):

$$VaCa(t) + VdCd(t) = VdCd(0)(1 - R) \quad (1)$$

$$P_e = -\frac{2.303Vd}{A(t - \tau_{lag})}\left(\frac{1}{1 + r_v}\right)\log_{10}\left[1 - \left(\frac{1 + r_v^{-1}}{1 - R}\right)\frac{Ca(t)}{Cd(0)}\right] \quad (2)$$

where *Va* is the volume of acceptor wells (cm^3)−300 μL; *Vd* (300 μL) is the volume of donor wells (cm^3); *A* (25 cm^3) is the filtration area (cm^2); *t* is time of incubation (*s*); *Cd*(*t*) and *Ca*(*t*) are the concentration of compound in donor and acceptor wells at time *t* (μM), respectively; *Cd*(0) is the concentration of compound in donor well at time 0 (μM); τ_{lag} is the

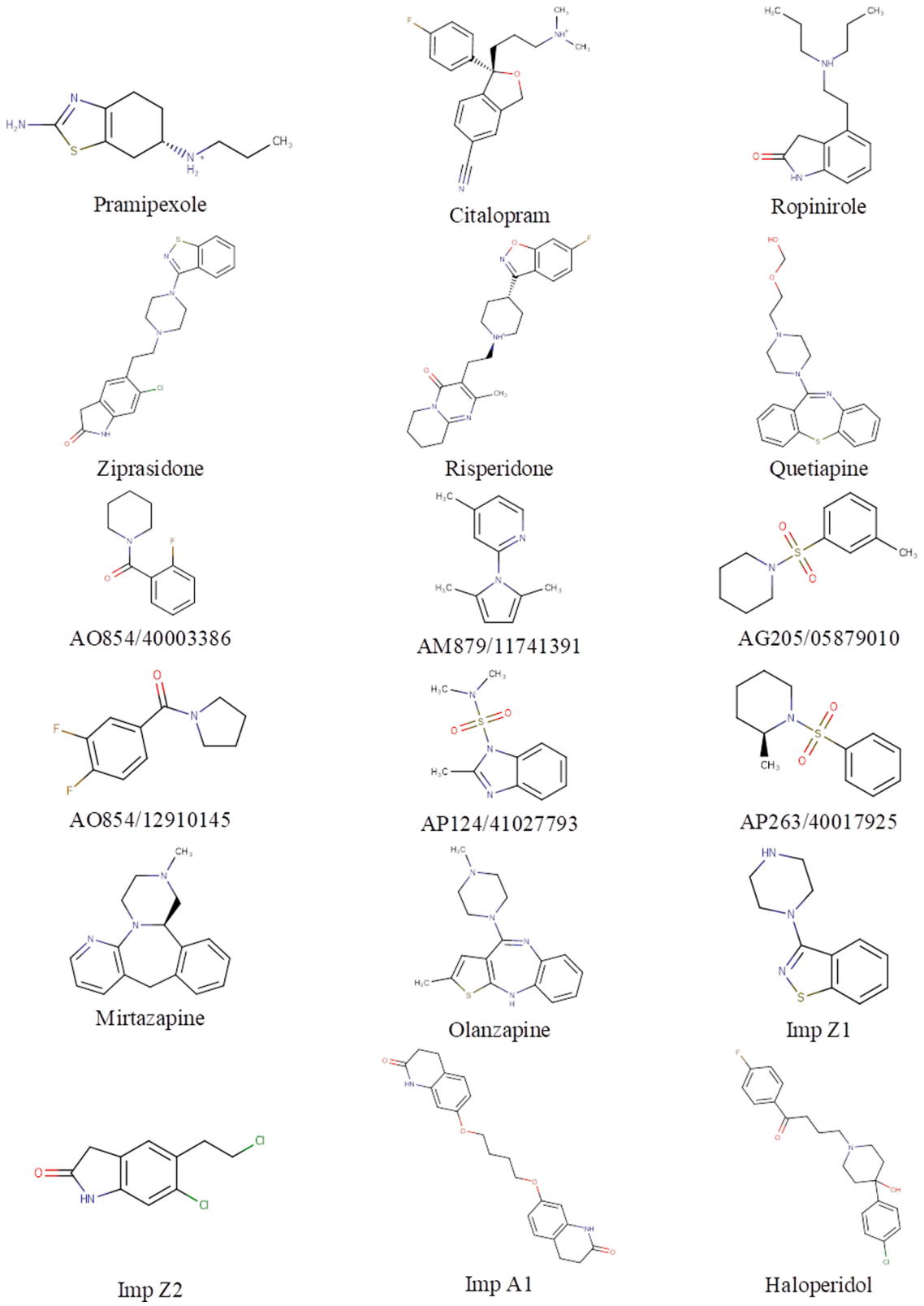

Fig. 1. The chemical structures of compounds used in the study.

time needed to saturate the membrane (approximately 20 min) (Avdeef et al., 2001); *R* is mole fraction of compound retained by membrane; and parameter r_v is calculated from the formula $r_v = Vd / Va$.

2.3. HPLC analysis for PAMPA assay

The HPLC analysis was carried out using previously developed method (Di et al., 2003; Vucicevic et al., 2015) with some mobile phase modification in order to achieve better separation. It was performed at

the room temperature using the Agilent Technologies 1200 HPLC system (Santa Clara, CA, USA) consisting of the UV detector. Chromatographic analysis was performed on Zobrax Eclipse Plus C18 column, 250 × 4.6 mm, with particle size 5 μm (Agilent Technologies, Waldbronn, Germany). The samples were injected through the Rheodyne injector valve with a 20 μL sample loop. The flow rate was set to 1 mL min^{-1}. The UV detection was carried out at 254 nm. A mobile phase of acetonitrile-ammonium acetate buffer (pH=3.9, 25 mM) at various percentages was used for hDAT substrates, while mixture of methanol-ammonium acetate buffer at various percentages was used for the CNS drugs and their related compounds (Kirchherr and Kuhnvelten, 2006; Vucicevic et al., 2015).

2.4. Computational method

For all examined compounds selection of dominant forms at physiological pH = 7.40 was performed in Marvin Sketch 5.5.1.0 programme (ChemAxon, 2011). Subsequently, dominant forms of all compounds were preoptimized by use of Gaussian (Frisch et al., 2009) semiempirical PM3 (Parameterized Model revision 3) method (Stewart, 1989a, 1989b), included in ChemBio3D Ultra 13 programme (CambridgeSoft Corporation, 2013), while Hartree-Fock / 3–21 G method (Wiberg, 1986) was used for more precise geometry minimisation.

2.5. Calculated molecular descriptors

Every QSPR approach requires diverse data set of molecular descriptors which contains chemical information about molecular structure in numeric form. They represent most significant features that are used in QSPR study for structure-property correlations. Reliable prediction of molecular descriptors is important for developing predictable models (Danishuddin and Khan, 2016). In the present work, we have created QSPR models using a set of geometrical, topological, electronical and physicochemical descriptors of the optimized structures, calculated using Dragon 6.0 (TALETE Srl., 2010) and ADMET Predictor 9.5 programmes (Simulation Plus Inc, 2019). Descriptors with zero or near zero variance were not included in model building. Additionally, Dragon software was used to select descriptors with intercorrelation lower than 0.99 (for partial least squares regression (PLS) model) or lower than 0.90 (for support-vector machines (SVM) and multiple linear regression (MLR) models) for model building (Dobričić et al., 2014; Vucicevic et al., 2015). Pairs of descriptors with intercorrelation higher than 0.90 for MLR and SVM and 0.99 for PLS were selected and those with stronger influence on dependant variable were kept for model development. The unit variance (UV) scaling was used as scaling procedure, and final set of 1484 calculated molecular descriptors was further used for model development. The SMILES structures of studied ligands along with PAMPA results and calculated descriptors are provided in the supplementary file.

2.6. QSPR modelling

The QSPR method can be described as an application of mathematical and statistical methods in order to find empirical relationship (QSPR models) between effective BBB permeability (logarithm of effective permeability - logP_e) and calculated structural parameters (molecular descriptors) of examined compounds.

The dependant variable (Y) represents the response being modelled, logP_e, while X_1, X_2, X_3 … X_n are the independent variables denoting different structural features or physicochemical properties of examined compounds. In this study, predictive QSPR models were developed using three different statistical methods: stepwise MLR, PLS, and SVM. Artificial neural network (ANN) analysis was not performed due to the relatively small size of the data set because it can affect the quality of the created model.

Two components which are the most important for obtaining the quantitative data are the dependant and independent variables. PLS and stepwise MLR are the representative techniques which are used for developing the linear regression model, whereas non-linear approaches include SVM analysis. The PLS study was performed in the Soft independent Modelling of Class Analogy SIMCA P + 12.0 programme (Umetrics AB, 2008) and variable importance in projection (*VIP*) score was used for variable selection, while stepwise MLR and SVM models were built using STATISTICA 13.6 (StatSoft Inc., 2019).

Initially, the whole data set (n = 18) was divided into training set of twelve compounds (pramipexole, citalopram, ropinirole, risperidone, AP263/40017925, AM879/11741391, AG205/05879010, AO854/12910145, ziprasidone, olanzapine, Imp Z2, haloperidol) and test set of six compounds (mirtazapine, AO854/40003386, AP124/41027793, quetiapine, Imp Z1, Imp A1) based on a PCA score plot, obtained using SIMCA P + 12.0. Compounds for the test set were selected from the PCA plot so that every test set compound remains near at least one of the training set compounds considering that logP_e values were homogeneously distributed in the whole range (Roy et al., 2015b). In order to provide relevant comparison between developed QSPR models, the same training and test set were used for all of them.

2.7. Model validation

The main aim of every QSPR study is development of validated model, so it can be used for predictive purposes. OECD principles (http://www.oecd.org/chemicalsafety/risk-assessment/37849783.pdf) give the best guideline for developing reliable and reproducible QSPR model. Therefore, different validation techniques were applied to check the predictivity of the created models.

The robustness and internal predictivity of the created models was examined by calculating parameters of internal validation such as *RMSEE* and Q^2_{LOO} Eqs. (3), ((4) and (5)). The calculation of these parameters is based on the compounds used in the model development (training set) according to following relationships:

$$PRESS = \sum_{i=1}^{n} e_{(i)}^2 \tag{3}$$

$$RMSE = \sqrt{\frac{PRESS}{n}} \tag{4}$$

$$Q^2 = 1 - \frac{PRESS}{\sum \left(Y_{obs(training)} - \overline{Y_{training}} \right)^2} \tag{5}$$

where validation parameters *PRESS* (Predicted Sum of Squares) and *RMSE* (*RMSEE* and *RMSEP*) are defined with parameter $e_{(i)}$. The $e_{(i)}$ represents the difference between observed and the predicted Y values, while n is the number of compound in training/test set.

From Eq. (5), the parameter $Y_{obs(training)}$ is an observed logP_e value for the compounds in training set, while $Y_{training}$ is average logP_e value of compounds from training set. For $Q^2 > 0.50$, it can be assumed that obtained QSPR model has a good predictivity power (Ojha and Roy, 2011; Roy et al., 2015b; Tropsha, 2010).

Even though, created models have high value of Q^2, it is insufficient condition for model to have high predictive power (Golbraikh and Tropsha, 2002; Tropsha, 2010). Prediction of the BBB permeability for a new set of compounds is one of the most important objectives. Therefore, it is crucial to emphasize that the real predictive capability of each created model can be verified only through external model validation which is employing the test set molecules.

External validation parameter R^2_{pred} is used for assessing the predictive power of the obtained models and reflects the degree of correlation between the observed and predicted data of the test set. It is calculated according to the following Eq. (6):

$$R^2_{pred} = 1 - \frac{PRESS}{\sum \left(Y_{obs(test)} - \overline{Y_{training}}\right)^2} \quad (6)$$

where $Y_{obs(test)}$ is an observed logP_e value for the test set compounds and $Y_{training}$ is average logP_e value of the training set compounds. The *PRESS* value is calculated for test set according to Eq. (3). High predictive potential of QSPR model could be expected if R^2_{pred} is higher than 0.50 (Golbraikh and Tropsha, 2002; Ojha and Roy, 2011; Roy et al., 2015b). Even though R^2_{pred} parameter has been used for clarifying external predictivity of the model, there are some novel validation parameters which better reflect external predictive power such as r^2_{metric}.

In this study, due to small test set size, $r^2_{metrics}$ (r^2_m, r'^2_m, r^{-2}_m, and Δr^2_m) was applied on the entire data set for overall validation ($r_m{}^2_{overall}$) Ojha and Roy, 2011). This analysis is based on predicted values of test set and *LOO* predicted values of training set. Calculation of r^2_m and r'^2_m is presented in following Eqs. (7) and ((8):

$$r^2_m = r^2\left(1 - \sqrt{|r^2 - r_0^2|}\right) \quad (7)$$

$$r'^2_m = r^2\left(1 - \sqrt{\left|r^2 - r_0'^2\right|}\right) \quad (8)$$

where r is the correlation between predicted and experimentally obtained data, while the intercept r_0 is obtained by swiching the coordinate axes in the system. The values of correlation coefficients r^2_m, and r'^2_m should be close and greater than 0.50 for an acceptable QSPR model, so as their average value (r^{-2}_m), while the difference between r^2_m, and r'^2_m (Δr^2_m) should be lower than 0.20 (Golbraikh and Tropsha, 2002; Ojha et al., 2011; Ojha and Roy, 2011).

As Ojha and Roy in 2011 introduced in their study, the advantages of overall r_m analysis is statistics based on prediction of larger number of compounds, which is really helpful for data sets with small test size. Another advantage is possibility of use this $r^2_{moverall}$ statistics for selecting the final model amongst comparable (Ojha and Roy, 2011).

Additionally, the model reliability was checked by calculating the Concordance correlation coefficient (*CCC*) according to this Eq. (9):

$$\overline{\rho}_c = \frac{2\sum_{i=1}^{n}\left(X_{obs(test)} - \overline{X}_{obs(test)}\right)\left(Y_{pred(test)} - \overline{Y}_{pred(test)}\right)}{\sum_{i=1}^{n}\left(X_{obs(test)} - \overline{X}_{obs(test)}\right)^2 + \sum_{i=1}^{n}\left(Y_{pred(test)} - \overline{Y}_{pred(test)}\right)^2 + n\left(\overline{X}_{pred(test)} - \overline{Y}_{pred(test)}\right)} \quad (9)$$

where the parameters $x_{obs(test)}$ and $y_{pred(test)}$ present observed and predicted values of the test compounds respectively, and n is the number of chemicals. The ideal value of *CCC* value should be equal to 1 (Gramatica and Sangion, 2016; Roy et al., 2015b).

2.8. Applicability domain (AD)

The applicability domain (AD) must be defined in order to build reliable and acceptable QSPR model. It plays a critical role in the prediction of new molecules based on how similar they are to the compounds that were used for building the model (i.e. training set). Williams's plot of standardized residuals versus leverages values (h_i) (Gramatica, 2007) was used to examine whether the compounds falls within the AD or outside of it (Roy et al., 2015a). The value of warning leverage h^* was calculated as follows

$$h^* = 3(p+1)/n \quad (10)$$

where p presents the number of model variables and n is the number of compounds in training set (Eq. (10)). If the leverage value (h) of a molecule is higher than the threshold value (h^*) the prediction should be considered potentially unreliable because it is out of the AD domain of the training set. SPSS v.18.0 software was used for this process (SPSS Inc., 2009).

2.9. SMD simulation

The use of molecular simulation to optimize lead compounds, accelerating the discovery of new drugs, remains a field of significant growth. Actually, several innovative computational techniques are nowadays available to predict the transport properties of molecules through membranes (Bemporad et al., 2004; Darve et al., 2008; Deng and Roux, 2009; Sotomayor and Schulten, 2007; Thai et al., 2020). In order to provide molecular insight into drug penetration through BBB, we have used a steered molecular dynamics method (Suan Li and Khanh Mai, 2012). All simulations were run using Nano Scale Molecular Dynamics (NAMD) software version 2.8 (Phillips et al., 2005), while the system was prepared with Visual Molecular Dynamics (VMD) (Humphrey et al., 1996). CHARMM-GUI Membrane Builder was used to generate a lipid bilayer (1,2-Dioleoyl-sn glycero-3-phosphocholine (DOPC)) for the simulation (Jo et al., 2008). The CGENFF web service (Vanommeslaeghe et al., 2009; Yu et al., 2012) was used to generate the topology file for the ligands. The system contained 3299 water molecules placed above and below the lipid bilayer, 72 DOPC molecules and one small compound. The complete system contained a total of ~ 19,890 atoms. The single molecule was inserted around 30 Å from the bilayer centre of mass, in the normal (z) direction. The Fig. 2 shows the schematic representation of the process studied in this article. The equilibrated system was used as the starting point for the SMD simulation. The pressure was 1 atmosphere, and the temperature was kept constant at 310 K. The pulling velocity was set to 10 Å/ns, while the force constant was set to 5 kcal/molÅ^2. The time step was set as 1 fs. The time of SMD simulations was different (13–20 ns), based on the exit route of the ligand. In order to prevent the system from drifting under the applied force, we have applied restraints to lipid heads, while the motion of molecule was limited to a cylinder within 8 Å of the central axis of the membrane. For each simulation, the molecule was pulled from bulk water, through the entire DOPC membrane, and out into bulk water again, in the direction of the z axis (Fig. 2) (Thai et al., 2020).

3. Results and discussion

3.1. PAMPA results

This study involved PAMPA-BBB technique for the determination of passive permeability through BBB. A set of six novel potential hDAT substrates and twelve CNS standards was examined in order to determine their effective permeability (logP_e), which was calculated using the measured concentration. High logP_e values correspond to high permeability through barrier and opposite. PAMPA results and available experimental log*BB* values from literature are shown in Table 1. Based on the obtained results it can be seen that ropinirole has a lower experimental BBB permeability (logBB = −0.30) which is consistent

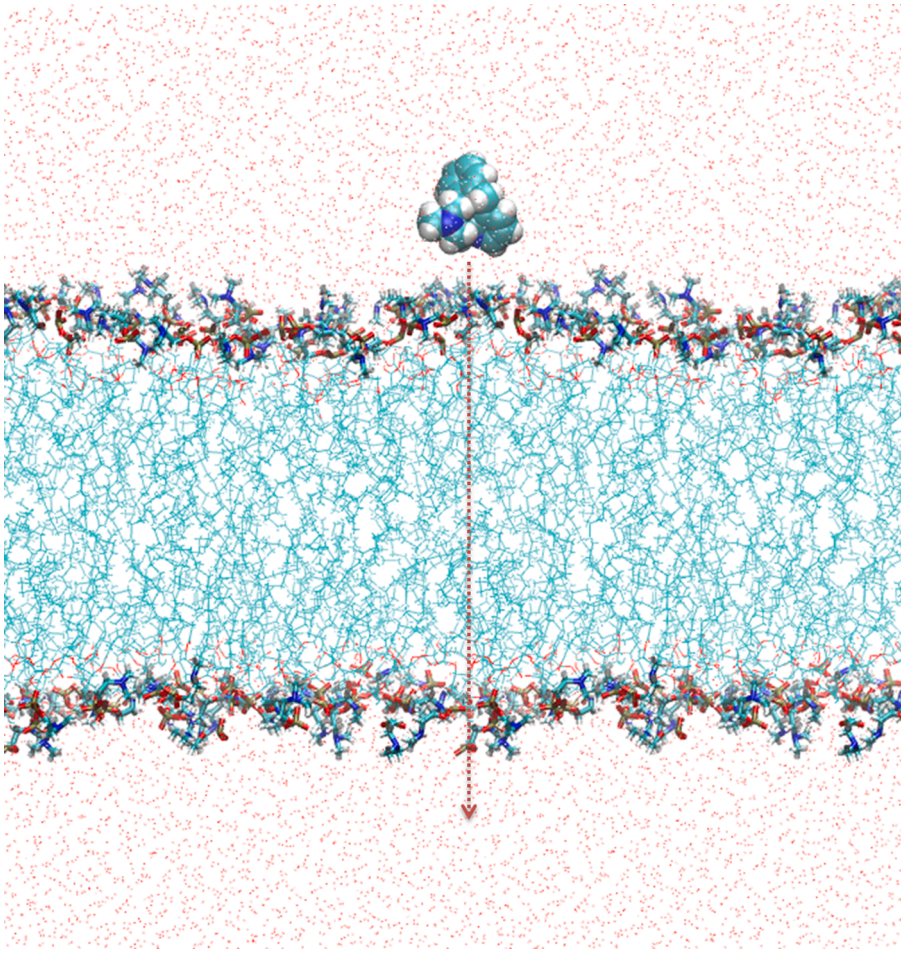

Fig. 2. Schematic representation of BBB penetration employing SMD method.

Table 1
Obtained PAMPA results.

Compound	logBB_{exp}	P_e	logP_e
Pramipexole	–	5.19E-05	−4.29
Citalopram	0.99 (Uhr and Grauer, 2003)	2.68E-04	−3.57
Ropinirole	−0.30 (Garg and Verma, 2006)	2.97E-05	−4.44
Mirtazapine	0.53 (Kelder et al., 1999)	2.42E-04	−3.54
Risperidone	−0.02 (Garg and Verma, 2006)	2.15E-04	−3.67
AP263/40017925	–	3.28E-04	−3.66
AO854/40003386	–	4.10E-04	−3.47
AM879/11741391	–	3.69E-04	−3.38
AG205/05879010	–	3.21E-05	−4.45
AO854/12910145	–	3.45E-04	−3.46
AP124/41027793	–	3.69E-04	−3.43
Quetiapine	–	1.67E-05	−4.78
Ziprasidone	–	1.08E-06	−5.88
Olanzapine	0.33 (Wang et al., 2004)	1.22E-04	−3.85
Imp Z1	–	4.67E-05	−4.42
Imp Z2	–	1.04E-04	−3.98
Imp A1	–	1.64E-04	−3.79
Haloperidol	1.34 (Sunderland and Cohen, 1987)	1.70E-04	−3.65

with lower logP_e value (−4.44), comparing to other molecules. Opposite, the citalopram and mirtazapine have a higher experimental logBB (citalopram = 0.99, mirtazapine = 0.53) and also a higer logP_e value (citalopram = −3.57; miratazapine = −3.54).

Following classification schemes reported in the literature (Bennion et al., 2017), molecules could be classified into four groups, using calculated experimental permeability rates (logP_e): impermeable compounds (logP_e < −6.14), low permeability compounds (−6.14 < logP_e < −5.66), medium permeability compounds (−5.66 < logP_e < −5.33) and high permeability compounds (logP_e > −5.33).

Using these cut-offs, we can conclude that all new potential neuroprotective drugs for Parkinson's disease, as well as all examined CNS drugs and related compounds, except ziprasidone, showed high BBB permeability due to high logP_e values (logP_e > −5.33). Ziprasidone was the only compound classified as low permeable (−6.14 < logP_e (−5.88) < −5.66).

In order to predict the potential effect of P-gp upon brain exposure to the studied drug candidates, an analysis was performed employing ADMET Predictor software (Simulation Plus Inc, 2019). Table S1 shows obtained results which indicate that neither hDAT substrates nor some CNS standards (pramipexole, risperidone, haloperidol, ziprasidone impurities) were identified as a substrates for P-gp. On the other hand, three compounds (citalopram, quetiapine and ziprasidone) were predicted as P-gp inhibitors, while the others were identified as substrates and not inhibitors (ropinirole, mirtazapine, olanzapine, Imp A1). Although it was predicted that efflux by P-gp may contribute to the limited penetration through BBB of some compounds, their intrinsic passive permeability may be sufficient for a satisfactory unbound concentration of drug in the brain (Summerfield et al., 2015). Moreover, to validate our PAMPA method, levodopa was used as control compound. Samples were analysed in triplicate and obtained results showed that levodopa was not detected in any of three acceptors cells, while it was in donor cells. On the whole, this indicates that PAMPA method could be used to effectively examine passive BBB permeability of examined compounds as well as to predict their potential efficiency in CNS.

Since selected hDAT ligands were not identified as substrates for P-gp, and showed remarkable results in PAMPA assay, logP_e ≥ −4.45, we

may conclude that these compounds could effectively penetrate BBB to achieve their neuroprotective effect in CNS.

3.2. Stepwise MLR, PLS and SVM modelling

Results obtained through PAMPA study were further employed for QSPR modelling with the aim of creating predictable *in silico* models for BBB permeability. In this study, a set of descriptors was calculated for each selected compound using ADMET predictor and Dragon programmes. Choosing the most significant molecular parameters is very important because they are a unique characterisation of the molecular structure with influence on BBB permeability.

Three different statistical methods: stepwise MLR, PLS and SVM were employed to create predictable and reliable QSPR models in order to find the most significant molecular parameters (descriptors) for BBB permeability.

Firstly, stepwise MLR analysis was employed to estimate the linear relationship between calculated molecular parameters and coefficient of effective permeability ($\log P_e$) of examined compounds. Stepwise procedure was applied for descriptor selection. This method presents a combination of the forward and backward selection techniques and allows moving in both directions (Chowdhury and Turin, 2020). Forward selection was used to start the process where independent variables were added to the model and evaluated at each step based on their statistical significance. If variable was found to be nonsignificant, it was removed from the model. Basically, this selection method evaluates variables at each step, adding or deleting them based on *F* to enter and *F* to remove criteria. In order to avoid over-fitting of the created MLR model, the predictive capabilities were examined by applying LOO cross-validation and obtained statistical parameters are shown in Table 2.

PLS is also a widely used method for determination of linear relationship between two sets of variables. Unlike MLR, PLS method can analyse numerous independent variables with stronger collinearity. *VIP* parameter was used to measure the importance of each molecular parameter. The variables with higher value of *VIP* coefficient show that they are more relevant to predict dependant variable and explain BBB permeability. The independent variables with *VIP* score larger than 1 are the most relevant for explaining *Y* value. Those X variables with $1.0 > VIP > 0.5$ are moderately influential while variables which have VIP value smaller than 0.5 are irrelevant for the model (Eriksson et al., 2006). Therefore, independent variables with lowest VIP score values were successively removed from the model. For every new PLS model statistical parameters were recalculated and procedure was repeated until best model was created. Reliability and robustness of formed PLS model was evaluated by permutation testing (Y scrambling). *Y* matrix was randomly reordered 100 times, while *X* matrix was kept unchanged. New model was recalculated and two separate intercepts were obtained, $R^2_{\text{int}} = -0.0024$ and $Q^2_{\text{int}} = -0.24$. Reliable model should have $R^2_{\text{intercept}} < 0.40$ and $Q^2_{\text{intercept}} < 0.05$ (Eriksson et al., 2006). The optimal QSPR-PLS model with one significant component ($A = 1$), relating two variables (SolvEMt_3D and H_0p) was selected. Calculated statistical parameters are shown in Table 2.

Since PLS model showed better reliability and predictability compare to stepwise MLR model (Table 2), the descriptors previously selected by PLS method were introduced as input variables to establish SVM modelling.

SVM is machine learning technique which can solve problems of small samples and nonlinearity (Golmohammadi et al., 2017). The SVM performance depends on several factors, such as the capacity parameter C, Kernel parameter γ, the epsilon ε and *Kernel* function. In this non-linear regression model, radial bias function (RBF) was selected as *Kernel* function. For optimization of *C*, ε and γ parameters their values were changed in the range of 10–45 for *C*, 0.01–0.10 for ε and 0.10–1.00 for γ to reach the less possible RMSE of 10-fold cross validation (Golmohammadi et al., 2017). According to the obtained results the best values for *C*, ε and γ were: 43, 0.09 and 0.125 respectively, and the number of support vectors in final model was 5. Parameters of statistical validation are listed in Table 2.

3.3. Interpretation of QSPR modelling

Calculated statistical parameters of different QSPR models (PLS, stepwise MLR and SVM) are presented in Table 2. The comparison of predictive abilities of created QSPR models indicated that SVM model is superior over PLS and MLR models due to better internal and external statistical parameters. The results showed that non-linear SVM model provides the best predictive capability and could be used to explain the relationship between BBB permeability and structural parameters of the examined compounds.

Stepwise MLR method was used for variable selection and prediction of linear relationship between molecular parameters and $\log P_e$ of tested compounds. It was found that lipophilicity (ALOGP2, squared Ghose-Crippen octanol-water partition coefficient) and solvation energy (SolvEMt_3D, length of the solvation energy moment vector) have a significant influence on BBB permeability. A negative coefficient of lipophilicity expressed as ALOGP2 implies that the parabolic relation between this descriptor and $\log P_e$ values opens downward. The analysis revealed that decrease in permeability was observed for the compounds with very high (ziprasidone) but also with very low (pramipexole,

Table 3
The calculated values of selected descriptors with MLR method and predicted $\log P_e$ for the training and test set (*).

Compound	ALOGP2	SolvEMt_3D	$\log Pe_{\text{predicted}}$
Pramipexole	0.02	36.99	−4.12
Citalopram	4.67	24.99	−3.97
Ropinirole	1.96	37.81	−4.27
Risperidone	3.09	21.62	−3.74
AP263/40017925	7.65	12.90	−3.70
AM879/11741391	8.25	2.26	−3.35
AG205/05879010	8.27	20.07	−4.01
AO854/12910145	4.48	9.57	−3.38
Ziprasidone	18.14	54.51	−5.90
Olanzapine	10.34	10.77	−3.79
Imp Z2	5.78	36.07	−4.44
Haloperidol	15.11	5.11	−3.88
Mirtazapine*	9.58	2.27	−3.43
AO854/40003386*	5.60	9.50	−3.45
AP124/41027793*	2.26	13.24	−3.38
Quetiapine*	10.01	29.23	−4.45
Imp Z1*	4.69	7.20	−3.31
Imp A1*	8.88	34.81	−4.59

Table 2
QSPR models and statistical parameters.

Model	Regression equation	Q^2	R^2	*RMSEE*	R^2_{pred}	*RMSEP*	r^2_m	r'^2_m	r^{-2}_m	Δr^2_m	*k'*	*CCC*
MLR	$\log P_e = -2.78 - 0.04$ SolvEMt_3D $- 0.06$ ALOGP2	0.86	0.86	0.26	−0.10	0.55	/	/	/	/	/	/
PLS	$\log P_e = f$(SolvEMt_3D, H_0p)	0.58	0.73	0.39	0.64	0.32	0.69	0.44	0.57	0.25	0.99	0.86
SVM	$\log P_e = f$(SolvEMt_3D, H_0p)	0.78	0.81	0.32	0.57	0.35	0.72	0.55	0.63	0.12	0.98	0.98
Criteria		> 0.50	> 0.70		> 0.50	≤ 2**RMSEE*	>0.50	>0.50	>0.50	<0.20	$0.85 \le k' \le 1.15$	≈ 1

Table 4
The calculated values of selected descriptors with PLS method and predicted logP_e for the training and test set (*).

Compound	H_0p	SolvEMt_3D	log$Pe_{predicted}$
Pramipexole	1.25	36.99	−4.27
Citalopram	1.33	24.99	−4.14
Ropinirole	1.16	37.81	−4.13
Risperidone	1.27	21.62	−3.97
AP263/40017925	1.21	12.90	−3.67
AM879/11741391	1.13	2.26	−3.30
AG205/05879010	1.28	20.07	−3.95
AO854/12910145	1.05	9.57	−3.32
Ziprasidone	1.79	54.51	−5.56
Olanzapine	1.37	10.77	−3.90
Imp Z2	1.49	36.07	−4.65
Haloperidol	1.33	5.11	−3.69
Mirtazapine*	1.24	2.27	−3.48
AO854/40003386*	1.11	9.50	−3.42
AP124/41027793*	1.27	13.24	−3.77
Quetiapine*	1.31	29.23	−4.21
Imp Z1*	1.51	7.20	−4.05
Imp A1*	1.15	34.81	−4.05

ropinirole) values of this parameter (Table 3). Nevertheless, created MLR model showed a very poor prognostic capability for external data set (Table 2), because of unsatisfied R^2_{pred} value ($R^2_{pred} < 0.50$) and very high error of prediction (*RMSEP*: 0.55).

The PLS model was created of two descriptors: H_0p (H autocorrelation of lag 0 / weighted by polarizability) and SolvEMt_3D. H_0p is Dragon descriptor, while SolvEMt_3D presents ADMET predictor descriptor. Calculated values of these descriptors are shown in Table 4. VIP values are 1.05 for SolvEMt_3D and 0.95 for H_0p (Fig. 3). According to the coefficient plot, both descriptors had negative influence on *Y* value (Fig. 4). Therefore, decreases in H_0p and SolvEMt_3D values of chemicals will increase the rate of brain penetration. Subsequently, descriptors selected by PLS model have been used for non-linear SVM model building.

The developed QSPR-SVM model (Table 5) was evaluated by internal and external validation parameters. Internal predictability of the created model was confirmed with high values of Q^2 and R^2 for training set compounds, while test set compounds were used to verify external predictability. Values of R^2_{pred}, r^2_m, r'^2_m, and r^{-2}_m greater than 0.50 and Δr^2_m lower than 0.20 specified that developed QSPR model had good predictive capability and could be used for the permeability prediction of new compounds. Due to better statistical values of external validation parameters, R^2_{pred} and $r_{metrics}$, SVM model has been selected as superior over PLS, as could be seen from Table 2. Choosing non-linear SVM model

Table 5
Results of QSPR- SVM model for the training and test set (*).

Compound	log$P_{e\ observed}$	log$P_{e\ predicted}$
Pramipexole	−4.29	−4.19
Citalopram	−3.57	−3.40
Ropinirole	−4.53	−4.10
Risperidone	−3.67	−3.84
AP263/40017925	−3.48	−3.60
AM879/11741391	−3.43	−3.39
AG205/05879010	−4.49	−3.82
AO854/12910145	−3.46	−3.39
Ziprasidone	−5.97	−5.85
Olanzapine	−3.91	−3.80
Imp Z2	−3.98	−4.57
Haloperidol	−3.77	−3.67
Mirtazapine*	−3.62	−3.51
AO854/40003386*	−3.39	−3.44
AP124/41027793*	−3.43	−3.68
Quetiapine*	−4.78	−4.08
Imp Z1*	−4.33	−4.00
Imp A1*	−3.79	−4.00

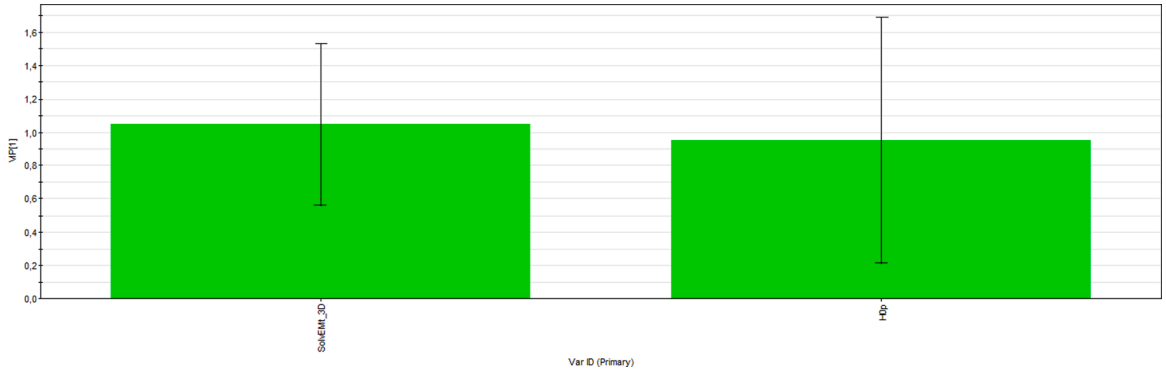

Fig. 3. VIP values of selected descriptors in created PLS model.

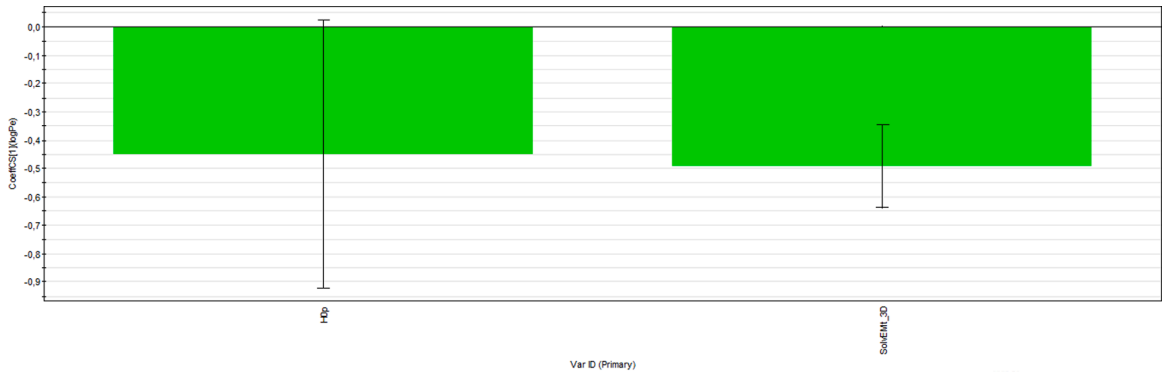

Fig. 4. Coefficient plot of selected descriptors in created PLS model.

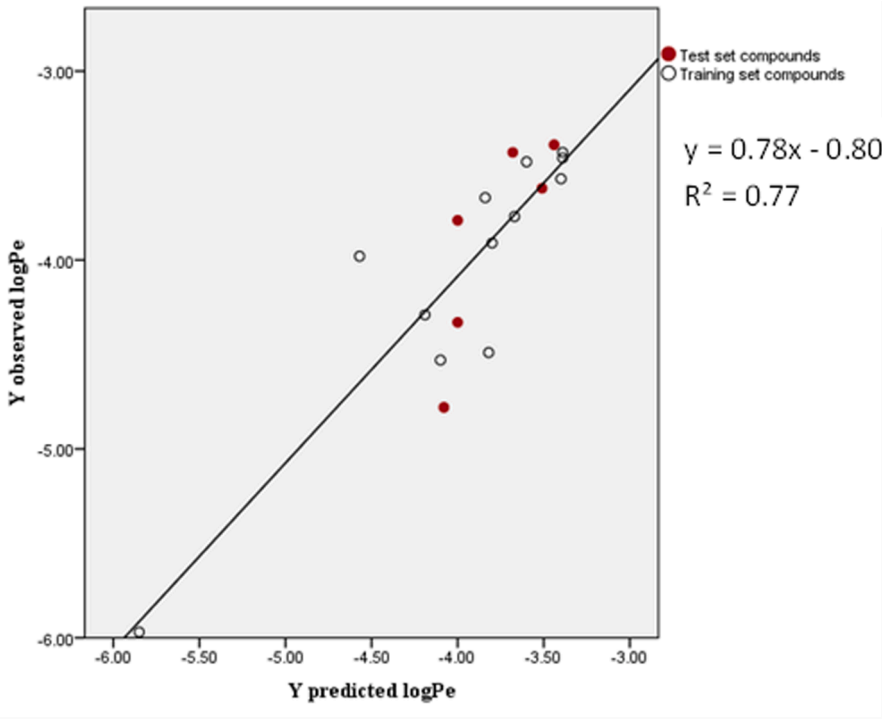

Fig. 5. The plot of observed versus predicted pKi values for the whole data for QSPR- SVM model.

as the best means that relation between significant descriptors (H_0p and SolvEMt_3D) and permeability (logP_e) is not absolutely linear. The plot of observed versus predicted logP_e values for the whole data set is shown in Fig. 5.

Interpretation of statistically significant descriptors could provide insight into molecular characteristics that are most important for BBB permeation and help us to understand which structural characteristics play an essential role in that process.

The H_0p belongs to H-GETAWAY descriptors (Consonni et al., 2002). It is calculated from molecular influence matrix H and contains geometrical and topological information expressed as a function of molecular weight, polarizability, VdW volume, and electronegativity, Eq. (11) (Consonni et al., 2002; Todeschini and Consonni, 2009a):

$$H_0(\mathrm{w}) = \sum_{i=1}^{A} h_{ii} \times w_i^2 \tag{11}$$

where h_{ii} are the off-diagonal elements of the molecular influence matrix H and w defines an atomic weighting scheme. In this case H_0p is 3D descriptor which takes into account the position of atoms and assesses their weight by polarizability at topological distance 0 in the 3D molecular space.

Compounds with highest values of this descriptor are ziprasidone and its impurities 1 and 2, so as olanzapine, due to presence of sulphur and chlorine atoms. These atoms have highest polarizability values (Todeschini and Consonni, 2009b) and because of that highest impact on decreasing BBB permeability. The lowest values of this descriptor have compounds with highest permeability through BBB (AO854/12910145, AO854/40003386, AM879/11741391). It could be concluded that introduction of fluorine atom instead of chlorine and absence of sulphur atom in molecule will improve permeability through BBB. Also, replacement of sulphonamide functional group with amide group show positive influence on permeability. The descriptor H_0p takes into account 3D structure of molecules, and not just their polarity character. Moreover, ligand with methyl group on aromatic ring (molecule AG205/05879010) have lower logP_e and higher H_0p values than molecule which have methyl group on saturated heterocyclic ring (AP263/40017925) due to different conformation of molecules.

SolvEMt_3D is 3D molecular descriptor calculated by ADMET predictor programme. As it has negative influence on Y value, the increase of the value of this descriptor will cause the decrease of permeability through BBB. This can be explain that compounds which have more polar groups and protonated nitrogen atom have higher values of SolvEMt_3D and lower BBB permeation (ziprasidone, ropinirole), but also 3D geometry of molecule should be considered.

In the current study, novel CNS drugs candidates were investigated and so far there is no QSPR study available for the selected data set in the literature. Presence of SolvEMt_3D and H_0p descriptors in created model revealed that topological aspects, 3D geometry, and polarizability of investigated compounds have significant influence on their BBB permeability. These categories of descriptors are important for developing predictable and reliable QSPR model. Suggested structural modifications presented above could be used for further optimisation of examined ligands in order to improve their BBB permeability. Besides, by using developed QSPR-SVM model permeability of structurally related CNS compounds or their impurities may be predicted if they are placed in the applicability domain of the created model. Furthermore, comparison between the created model and the models in the literature has been described on the basis of molecular descriptors that play a critical role in defining BBB permeability. Zhang et al. through application of combinatorial quantitative structure activity relationship (QSAR) approach revealed that despite lipophilicity, hydrogen-bonding properties and polar surface area, E-state and van der Waals surface areas (VSA) also show significant influence on permeability through BBB (Zhang et al., 2008). Additionally, Subramanian et al. reported that electrotopological descriptors are of significant interest (Subramanian and Kitchen, 2003), while Nikolic et al. highlighted the importance of hydrophilicity and GETAWAY descriptors (Nikolic et al., 2013). Also, some other descriptors have been described to be important in predicting the BBB permeability of drugs, such as polarizability and electronegativity (Abraham et al., 1995; Vucicevic et al., 2015). These results are in agreement with our observations when comparing which descriptors mainly affect the BBB permeability.

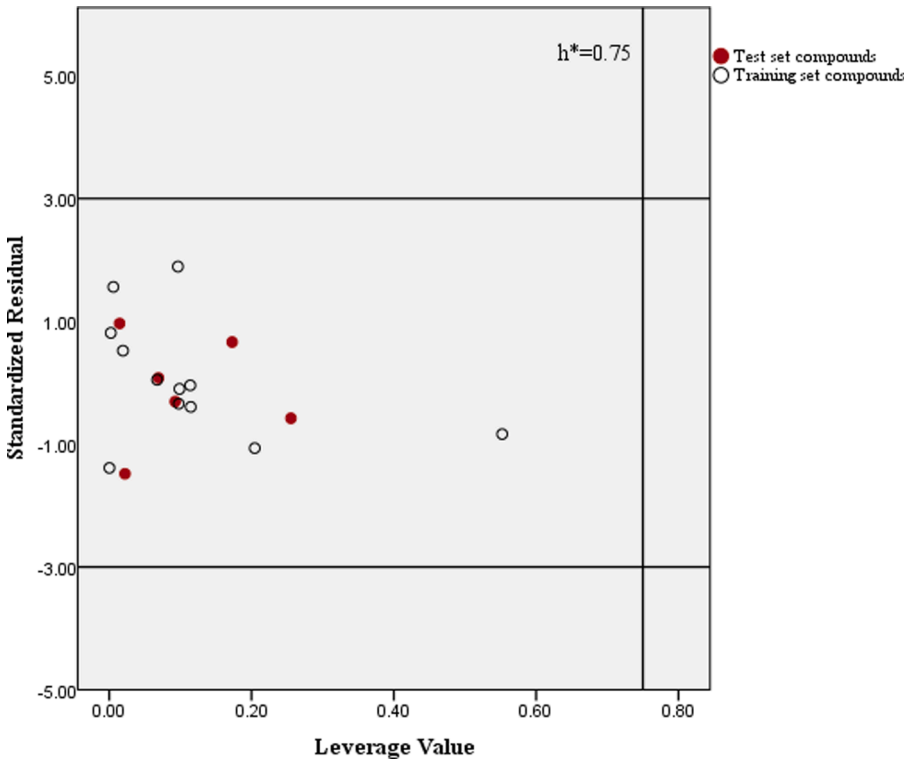

Fig. 6. Applicability domain of the created QSPR-SVM model.

3.4. Applicability domain of developed QSPR models

The most important variables from created PLS and SVM models were used for defining their domain of applicability. Based on the previously mentioned Eq. (10) the warning leverage value was calculated ($h^* = 0.75$). The Williams Plot is presented in Fig. 6. The obtained results indicated that neither training nor test set compounds deviated from the defined AD. Therefore, we can conclude that created SVM model could be further used for predicting the BBB permeability of new, structurally similar compounds. In particular, it can be of great importance for optimisation of selected hDAT ligands in order to rationally design novel, more potent compounds.

3.5. SMD simulations

SMD methodology has been widely applied to the study of various processes, including ligand-protein binding, transport of compounds through membrane channels, ligands unbinding pathways, as well as exploring the permeability of ligands through membranes (Izrailev et al., 1999; Pakdel et al., 2020; Patel et al., 2014; Pedram et al., 2015; Shen et al., 2012; Thai et al., 2020). However, SMD technique in this article was employed to gain qualitative picture of the BBB permeation pathway for studied compounds. The system was set up as described in methodology section. Snapshots from the SMD simulation of the AM879/11741391 molecule at different positions relative to the DOPC bilayer are shown in Fig. 7. Correlation between force peaks and simulation time was studied using Excel for graph building and VMD for visualization of process.

In Figs. S1-S3, we reported the force profiles as a function of time obtained from SMD simulations for all studied compounds. At the beginning of each simulation the ligand is placed in the water which is represented by force peaks below 150 pN. After the ligand enters the lipid bilayer (t_1) force peaks are becoming higher and increases to maximum 385.88 pN for ropinirole. This increasing tendency in the force magnitude may be associated with the entering of the ligand in the hydrophobic tails of the lipid bilayer, and it is retained until the ligand comes out again to water phase. Consequently, the last high peak of the force–time curve (t_2) could be observed as the ligand leaves the polar heads of the second DOPC monolayer. After crossing the bilayer and entering to water again, force magnitude significantly decreases and

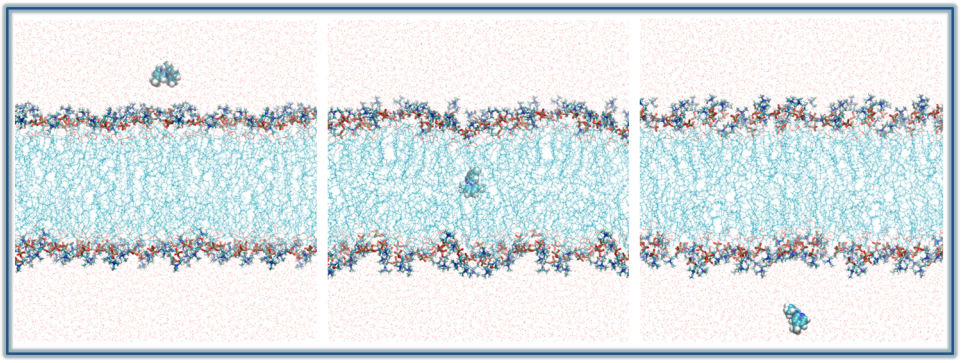

Fig. 7. SMD simulation of the AM879/11741391 molecule at different positions.

Table 6
Difference between two peaks selected on graphs (Figs. S1-S3) presenting time needed to cross the DOPC bilayer, the maximum force, F_{max}, and logP_e.

Compound	Time (ns)	F_{max} (pN)	logP_e
Pramipexole	6.20	240.44	−4.29
Citalopram	13.40	292.15	−3.57
Ropinirole	11.60	395.88	−4.44
Mirtazapine	8.20	226.51	−3.54
Risperidone	9.00	265.35	−3.67
AP263/40017925	8.50	265.47	−3.66
AO854/40003386	7.40	183.10	−3.47
AM879/11741391	6.00	262.42	−3.38
AG205/05879010	8.40	293.09	−4.45
AO854/12910145	6.40	226.45	−3.46
AP124/41027793	8.40	281.11	−3.43
Quetiapine	12.20	334.69	−4.78
Ziprasidone	17.00	348.53	−5.88
Olanzapine	9.50	237.50	−3.85
Imp Z1	7.50	239.88	−4.42
Imp Z2	9.80	261.18	−3.98
Imp A1	8.90	317.60	−3.79
Haloperidol	10.00	352.50	−3.65

becomes more stable. Moreover, examined ligands were inspected in terms of time needed to cross the DOPC bilayer, calculating the time difference between two peaks selected on graphs (t_2 and t_1). Obtained results are presented in Table 6 and were compared with logP_e values from PAMPA study. Calculated value of correlation coefficient ($r_{time/logPe}$=0.66) indicates strongly negative correlation between examined values. Nevertheless, based on performed simulations it may be concluded that ziprasidone took the longest time (17 ns) to pass through the barrier (Fig. S3) while AM879/11741391 took the least time (6 ns) (Fig. S1), which is in concordance with logP_e values for these compounds. Since the force is the main output of the simulation, values of maximum force, F_{max}, applied on each compound are also reported in Table 6. Obtained results indicated moderately negative correlation ($r_{Fmax/logPe}$=- 0.50) between F_{max} and logP_e values from PAMPA study. Notably, as the maximum force increases the logP_e values decrease. This is the most evident in the examples of ropinirole, ziprasidone and quetiapine which possess the lowest logP_e values. Following these findings we can observed that the larger force have to be exerted on the low permeable compounds (logP_e < 5.66) to pass through the membrane.

The performed SMD simulations enabled us to gain deeper insight into BBB permeation pathway of studied compounds, providing information about the forces exerted on the compounds during the translocation process. Compared to the QSPR modelling which quantitative prediction of logP_e is limited to a narrow set of training-like compounds, MD simulations can be used as a reliable pre-screening method for relative permeability prediction of structurally different compounds. However, both of them present promising tools for a rapid and inexpensive permeability assessment of newly designed CNS compounds before synthesis and *in vitro* testing. Moreover, the main potential of this methodology is to be expanded in the future by utilization of performed SMD simulations as starting states for more complex free-energy calculations, such as umbrella sampling (Bennion et al., 2017).

4. Conclusion

In presented study, *in vitro* PAMPA technique was used for the prediction of BBB penetration of eighteen compounds, six novel potential hDAT substrates, twelve CNS approved drugs and their related compounds. Experimentally obtained permeability values (logP_e) and calculated molecular descriptors were used for performing QSPR analysis. Three different statistical methods (PLS, stepwise MLR, and SVM) were employed to develop linear and non-linear QSPR models for successful prediction of BBB permeability. The limitation of data set was solved with extensive statistical validation of the created models. The results emphasised that created SVM model showed great predictive capability based on the obtained values of Q^2, R^2_{pred}, $r_{metrics}$ and CCC parameters. Therefore, it can be effectively used to explain the relationship between selected structural descriptors and BBB permeability with high accuracy, as well as to predict the permeability of new designed analogues that are within of the defined applicability domain. H_0p and SolvEMt_3D are descriptors with the strongest influence on logP_e values. A decrease in their values will lead to an increase in logP_e, and consequently better permeability through BBB. Selected descriptors define topological aspects and 3D geometry of molecules and could be used to describe structural modifications in order to improve BBB permeability. Modifications such as replacement of the fluorine with chlorine, introduction of amide group instead of sulphonamide functional group and removal of sulphur atom in molecule could enhance BBB penetration of examined compounds. Furthermore, our future work will be based on the rational drug design of new hDAT ligands, while created QSPR model will be used not only to guide structural modifications, but also to offer some reference for experimental study in order to reduce the workload and save resources. In addition, SMD simulations have been carried out to visualize and explain an entire BBB permeation pathway therefore laying a good foundation for future *in silico* testing. Overall, consistency between results obtained through the integration of *in vitro* PAMPA technique with *in silico* computational methods enabled us to provide reliable, relatively quick and inexpensive methodology for assessment of brain penetration. Structural diversity of the data set compounds and external predictability of the created model provide the potential utility of these methods for permeability assessment through BBB of related CNS candidates and theirs impurities. Results obtained through this study demonstrated that novel hDAT substrates most likely cross the BBB by passive diffusion, which is very important for further studies of their neuroprotective effect in Parkinson's disease.

Credit author statement

Teodora Djikic, Milica Radan and Katarina Nikolic: Conceptualization and Methodology; Teodora Djikic and Milica Radan: Experimental and Computational work; Darija Obradovic: Experimental work (HPLC); Milica Radan: Writing- Original draft preparation.

Acknowledgments

The authors acknowledge the Ministry of Science and Technological Development of the Republic of Serbia, Faculty of Pharmacy UB Contract No. 451–03–9/2021–14/200161.

The authors would like to thank the European Cooperation in Science and Technology (COST) COST Actions CA18133 and CA18240.

Numerical simulations were run on the PARADOX-IV supercomputing facility at the Scientific Computing Laboratory, National center of Excellence for the Study of Complex Systems, Institute of Physics Belgrade, supported in part by the Ministry of Education, Science, and Technological Development of the Republic of Serbia.

Supplementary materials

Supplementary material associated with this article can be found, in the online version, at doi:10.1016/j.ejps.2021.106056.

References

Abbott, N.J., 2004. Prediction of blood–brain barrier permeation in drug discovery from in vivo, in vitro and in silico models. Drug Discov. Today Technol. 1, 407–416. https://doi.org/10.1016/j.ddtec.2004.11.014.

Abbott, N.J., Rönnbäck, L., Hansson, E., 2006. Astrocyte–endothelial interactions at the blood–brain barrier. Nat. Rev. Neurosci. 7, 41–53. https://doi.org/10.1038/nrn1824.

Abraham, M.H., Chadha, H.S., Mitchell, R.C., 1995. Hydrogen-bonding. Part 36. Determination of blood brain distribution using octanol-water partition coefficients. Drug Des. Discov. 13, 123–131.

Avdeef, A., 2005. The rise of PAMPA. Expert Opin. Drug Metab. Toxicol. 1, 325–342. https://doi.org/10.1517/17425255.1.2.325.

Avdeef, A., 2003. Permeability, in: absorption and Drug Development. Wiley 116–246. https://doi.org/10.1002/047145026X.ch7.

Avdeef, A., Strafford, M., Block, E., Balogh, M.P., Chambliss, W., Khan, I., 2001. Drug absorption in vitro model: filter-immobilized artificial membranes. Eur. J. Pharm. Sci. 14, 271–280. https://doi.org/10.1016/S0928-0987(01)00191-9.

Balestrino, R., Schapira, A.H.V., 2020. Parkinson disease. Eur. J. Neurol. 27, 27–42. https://doi.org/10.1111/ene.14108.

Bemporad, D., Essex, J.W., Luttmann, C., 2004. Permeation of Small Molecules through a Lipid Bilayer: a Computer Simulation Study. J. Phys. Chem. B 108, 4875–4884. https://doi.org/10.1021/jp035260s.

Bennion, B.J., Be, N.A., McNerney, M.W., Lao, V., Carlson, E.M., Valdez, C.A., Malfatti, M.A., Enright, H.A., Nguyen, T.H., Lightstone, F.C., Carpenter, T.S., 2017. Predicting a Drug's Membrane Permeability: a Computational Model Validated With in Vitro Permeability Assay Data. J. Phys. Chem. B 121, 5228–5237. https://doi.org/10.1021/acs.jpcb.7b02914.

Bicker, J., Alves, G., Fortuna, A., Falcão, A., 2014. Blood–brain barrier models and their relevance for a successful development of CNS drug delivery systems: a review. Eur. J. Pharm. Biopharm. 87, 409–432. https://doi.org/10.1016/j.ejpb.2014.03.012.

CambridgeSoft Corporation, 2013. ChemBio3D Ultra, Version 13.0. Cambridge, MA, USA.

Carpenter, T.S., Kirshner, D.A., Lau, E.Y., Wong, S.E., Nilmeier, J.P., Lightstone, F.C., 2014. A Method to Predict Blood-Brain Barrier Permeability of Drug-Like Compounds Using Molecular Dynamics Simulations. Biophys. J. 107, 630–641. https://doi.org/10.1016/j.bpj.2014.06.024.

ChemAxon, 2011. MarvinSketch 5.5.1.0. Budapest, Hungary.

Chowdhury, M.Z.I., Turin, T.C., 2020. Variable selection strategies and its importance in clinical prediction modelling. Fam. Med. Community Heal. 8, e000262 https://doi.org/10.1136/fmch-2019-000262.

Clark, D.E., 2003. In silico prediction of blood–brain barrier permeation. Drug Discov. Today 8, 927–933. https://doi.org/10.1016/S1359-6446(03)02827-7.

Consonni, V., Todeschini, R., Pavan, M., 2002. Structure/Response Correlations and Similarity/Diversity Analysis by GETAWAY Descriptors. 1. Theory of the Novel 3D Molecular Descriptors. J. Chem. Inf. Comput. Sci. 42, 682–692. https://doi.org/10.1021/ci015504a.

Danishuddin, Khan, A.U., 2016. Descriptors and their selection methods in QSAR analysis: paradigm for drug design. Drug Discov. Today 21, 1291–1302. https://doi.org/10.1016/j.drudis.2016.06.013.

Darve, E., Rodríguez-Gómez, D., Pohorille, A., 2008. Adaptive biasing force method for scalar and vector free energy calculations. J. Chem. Phys. 128, 144120 https://doi.org/10.1063/1.2829861.

Deng, Y., Roux, B., 2009. Computations of Standard Binding Free Energies with Molecular Dynamics Simulations. J. Phys. Chem. B 113, 2234–2246. https://doi.org/10.1021/jp807701h.

Di, L., Kerns, E.H., Fan, K., McConnell, O.J., Carter, G.T., 2003. High throughput artificial membrane permeability assay for blood–brain barrier. Eur. J. Med. Chem. 38, 223–232. https://doi.org/10.1016/S0223-5234(03)00012-6.

Dickson, D.W., 2012. Parkinson's Disease and Parkinsonism: neuropathology. Cold Spring Harb. Perspect. Med. 2, a009258 https://doi.org/10.1101/cshperspect.a009258 a009258.

Djikic, T., Martí, Y., Spyrakis, F., Lau, T., Benedetti, P., Davey, G., Schloss, P., Yelekci, K., 2019. Human dopamine transporter: the first implementation of a combined in silico/in vitro approach revealing the substrate and inhibitor specificities. J. Biomol. Struct. Dyn. 37, 291–306. https://doi.org/10.1080/07391102.2018.1426044.

Dobričić, V., Marković, B., Nikolic, K., Savić, V., Vladimirov, S., Čudina, O., 2014. 17β-carboxamide steroids – in vitro prediction of human skin permeability and retention using PAMPA technique. Eur. J. Pharm. Sci. 52, 95–108. https://doi.org/10.1016/j.ejps.2013.10.017.

Eriksson, L., Kettaneh-Wold, N., Trygg, J., Wikström, C., Wold, S., 2006. Multi- and Megavariate Data Analysis : Part I: Basic Principles and Applications. Umetrics IncDepartment of Chemistry, Faculty of Science and Technology, Umeå University.

Frisch, M.J., Trucks, G.W., Schlegel, H.B., Scuseria, G.E., Robb, M.A., Cheeseman, J.R., Scalmani, G., Barone, V., Mennucci, B., Petersson, G.A., Nakatsuji, H., Caricato, M., Li, X., Hratchian, H.P., Izmaylov, A.F., Bloino, J., Zheng, G., Sonnenb, D.J., 2009. Gaussian 09. Gaussian, Inc, Wallingford CT.

Garberg, P., Ball, M., Borg, N., Cecchelli, R., Fenart, L., Hurst, R.D., Lindmark, T., Mabondzo, A., Nilsson, J.E., Raub, T.J., Stanimirovic, D., Terasaki, T., Öberg, J.-O., Österberg, T., 2005. In vitro models for the blood–brain barrier. Toxicol. Vitr. 19, 299–334. https://doi.org/10.1016/j.tiv.2004.06.011.

Garg, P., Verma, J., 2006. In Silico Prediction of Blood Brain Barrier Permeability: an Artificial Neural Network Model. J. Chem. Inf. Model. 46, 289–297. https://doi.org/10.1021/ci050303i.

Golbraikh, A., Tropsha, A., 2002. Beware of q2! J. Mol. Graph. Model. 20, 269–276. https://doi.org/10.1016/S1093-3263(01)00123-1.

Golmohammadi, H., Dashtbozorgi, Z., Khooshechin, S., 2017. Prediction of Blood-to-Brain Barrier Partitioning of Drugs and Organic Compounds Using a QSPR Approach. Acta Physico-Chimica Sin 33, 1160–1170. https://doi.org/10.3866/PKU.WHXB201704051.

Gramatica, P., 2007. Principles of QSAR models validation: internal and external. QSAR Comb. Sci. 26, 694–701. https://doi.org/10.1002/qsar.200610151.

Gramatica, P., Sangion, A., 2016. A Historical Excursus on the Statistical Validation Parameters for QSAR Models: a Clarification Concerning Metrics and Terminology. J. Chem. Inf. Model. 56, 1127–1131. https://doi.org/10.1021/acs.jcim.6b00088.

Humphrey, W., Dalke, A., Schulten, K., 1996. VMD: visual molecular dynamics. J. Mol. Graph. 14, 33–38. https://doi.org/10.1016/0263-7855(96)00018-5.

Izrailev, S., Stepaniants, S., Isralewitz, B., Kosztin, D., Lu, H., Molnar, F., Wriggers, W., Schulten, K., 1999. Steered Molecular Dynamics BT - Computational Molecular Dynamics: challenges, Methods, Ideas, in: Deuflhard, P., Hermans, J., Leimkuhler, B., Mark, A.E., Reich, S., Skeel, R.D. (Eds.), Springer Berlin Heidelberg, Berlin, Heidelberg, pp. 39–65.

Jo, S., Kim, T., Iyer, V.G., Im, W., 2008. CHARMM-GUI: a web-based graphical user interface for CHARMM. J. Comput. Chem. 29, 1859–1865. https://doi.org/10.1002/jcc.20945.

Kansy, M., Senner, F., Gubernator, K., 1998. Physicochemical High Throughput Screening: parallel Artificial Membrane Permeation Assay in the Description of Passive Absorption Processes. J. Med. Chem. 41, 1007–1010. https://doi.org/10.1021/jm970530e.

Kelder, J., Grootenhuis, P.D.J., Bayada, D.M., Delbressine, L.P.C., Ploemen, .J..-P., 1999. Polar Molecular Surface as a Dominating Determinant for Oral Absorption and Brain Penetration of Drugs. Pharm. Res. 16, 1514–1519. https://doi.org/10.1023/A:1015040217741.

Kerns, E., Di, L., 2002. Multivariate Pharmaceutical Profiling for Drug Discovery. Curr. Top. Med. Chem. 2, 87–98. https://doi.org/10.2174/1568026023394470.

Kirchherr, H., Kuhnvelten, W., 2006. Quantitative determination of forty-eight antidepressants and antipsychotics in human serum by HPLC tandem mass spectrometry: a multi-level, single-sample approach. J. Chromatogr. B 843, 100–113. https://doi.org/10.1016/j.jchromb.2006.05.031.

McHugh, P.C., Buckley, D.A., 2015. The Structure and Function of the Dopamine Transporter and its Role in CNS Diseases. pp. 339–369. https://doi.org/10.1016/bs.vh.2014.12.009.

Nielsen, P.A., Andersson, O., Hansen, S.H., Simonsen, K.B., Andersson, G., 2011. Models for predicting blood–brain barrier permeation. Drug Discov. Today 16, 472–475. https://doi.org/10.1016/j.drudis.2011.04.004.

Nikolic, K., Filipic, S., Smoliński, A., Kaliszan, R., Agbaba, D., 2013. Partial Least Square and Hierarchical Clustering in ADMET Modeling: prediction of Blood – Brain Barrier Permeation of α-Adrenergic and Imidazoline Receptor Ligands. J. Pharm. Pharm. Sci. 16, 622. https://doi.org/10.18433/J3JK5P.

Ojha, P.K., Mitra, I., Das, R.N., Roy, K., 2011. Further exploring rm2 metrics for validation of QSPR models. Chemom. Intell. Lab. Syst. 107, 194–205. https://doi.org/10.1016/j.chemolab.2011.03.011.

Ojha, P.K., Roy, K., 2011. Comparative QSARs for antimalarial endochins: importance of descriptor-thinning and noise reduction prior to feature selection. Chemom. Intell. Lab. Syst. 109, 146–161. https://doi.org/10.1016/j.chemolab.2011.08.007.

Pakdel, M., Raissi, H., Shahabi, M., 2020. Predicting doxorubicin drug delivery by single-walled carbon nanotube through cell membrane in the absence and presence of nicotine molecules: a molecular dynamics simulation study. J. Biomol. Struct. Dyn. 38, 1488–1498. https://doi.org/10.1080/07391102.2019.1611474.

Patel, J.S., Berteotti, A., Ronsisvalle, S., Rocchia, W., Cavalli, A., 2014. Steered Molecular Dynamics Simulations for Studying Protein–Ligand Interaction in Cyclin-Dependent Kinase 5. J. Chem. Inf. Model. 54, 470–480. https://doi.org/10.1021/ci4003574.

Pedram, M.Z., Shamloo, A., Alasti, A., Zadeh, E.G., 2015. Steered Molecular Dynamic Simulation Approaches for computing the Blood Brain Barrier (BBB) Diffusion Coefficient. pp. 1699–1703. https://doi.org/10.1007/978-3-319-19387-8_413.

Phillips, J.C., Braun, R., Wang, W., Gumbart, J., Tajkhorshid, E., Villa, E., Chipot, C., Skeel, R.D., Kalé, L., Schulten, K., 2005. Scalable molecular dynamics with NAMD. J. Comput. Chem. 26, 1781–1802. https://doi.org/10.1002/jcc.20289.

Roy, K., Kar, S., Ambure, P., 2015a. On a simple approach for determining applicability domain of QSAR models. Chemom. Intell. Lab. Syst. 145, 22–29. https://doi.org/10.1016/j.chemolab.2015.04.013.

Roy, K., Kar, S., Das, R.N., 2015b. Statistical Methods in QSAR/QSPR. Springer, Cham, pp. 37–59. https://doi.org/10.1007/978-3-319-17281-1_2. A Primer on QSAR/QSPR Modeling.

Shen, Z., Cheng, F., Xu, Y., Fu, J., Xiao, W., Shen, J., Liu, G., Li, W., Tang, Y., 2012. Investigation of Indazole Unbinding Pathways in CYP2E1 by Molecular Dynamics Simulations. PLoS ONE 7, e33500. https://doi.org/10.1371/journal.pone.0033500.

Simulation Plus Inc, 2019. ADMET Predictor 9.5. Lancaster, CA, USA.

Sotomayor, M., Schulten, K., 2007. Single-Molecule Experiments in Vitro and in Silico. Science 316, 1144–1148. https://doi.org/10.1126/science.1137591, 80-.

SPSS Inc., 2009. PASW Statistics for Windows. Version 18.0. Chicago: SPSS Inc.

StatSoft Inc, 2019. Statistica," Data Analysis Software System version 13.6.

Stewart, J.J.P., 1989a. Optimization of parameters for semiempirical methods I. Method. J. Comput. Chem. 10, 209–220. https://doi.org/10.1002/jcc.540100208.

Stewart, J.J.P., 1989b. Optimization of parameters for semiempirical methods II. Applications. J. Comput. Chem. 10, 221–264. https://doi.org/10.1002/jcc.540100209.

Suan, Li.M., Khanh Mai, B., 2012. Steered Molecular Dynamics-A Promising Tool for Drug Design. Curr. Bioinform. 7, 342–351. https://doi.org/10.2174/157489312803901009.

Subramanian, G., Kitchen, D.B., 2003. Computational models to predict blood–brain barrier permeation and CNS activity. J. Comput. Aided. Mol. Des. 17, 643–664. https://doi.org/10.1023/B:JCAM.0000017372.32162.37.

Sugano, K., 2007. Artificial Membrane Technologies to Assess Transfer and Permeation of Drugs in Drug Discovery. Comprehensive Medicinal Chemistry II 453–487. https://doi.org/10.1016/B0-08-045044-X/00136-X. Elsevier.

Summerfield, S., Jeffrey, P., Sahi, J., Chen, L., 2015. Passive Diffusion Permeability of the BBB-Examples and SAR, in: Blood-Brain Barrier in Drug Discovery. John Wiley & Sons, Inc, Hoboken, NJ, pp. 95–112. https://doi.org/10.1002/9781118788523.ch5.

Sun, H., Nguyen, K., Kerns, E., Yan, Z., Yu, K.R., Shah, P., Jadhav, A., Xu, X., 2017. Highly predictive and interpretable models for PAMPA permeability. Bioorg. Med. Chem. 25, 1266–1276. https://doi.org/10.1016/j.bmc.2016.12.049.

Sunderland, T., Cohen, B.M., 1987. Blood to brain distribution of neuroleptics. Psychiatry Res 20, 299–305. https://doi.org/10.1016/0165-1781(87)90090-4.
Szekely, G., Amores de Sousa, M.C., Gil, M., Castelo Ferreira, F., Heggie, W., 2015. Genotoxic Impurities in Pharmaceutical Manufacturing: sources, Regulations, and Mitigation. Chem. Rev. 115, 8182–8229. https://doi.org/10.1021/cr300095f.
TALETE Srl, 2010. Dragon.
Thai, N.Q., Theodorakis, P.E., Li, M.S., 2020. Fast Estimation of the Blood–Brain Barrier Permeability by Pulling a Ligand through a Lipid Membrane. J. Chem. Inf. Model. 60, 3057–3067. https://doi.org/10.1021/acs.jcim.9b00834.
Todeschini, R., Consonni, V., 2009a. Molecular Descriptors for Chemoinformatics: A, in: methods and Principles in Medicinal Chemistry. Wiley 1–38. https://doi.org/10.1002/9783527628766.ch1.
Todeschini, R., Consonni, V., 2009b. Molecular Descriptors for Chemoinformatics: G, in: methods and Principles in Medicinal Chemistry. pp. 325–366. https://doi.org/10.1002/9783527628766.ch7.
Tropsha, A., 2010. Best Practices for QSAR Model Development, Validation, and Exploitation. Mol. Inform. 29, 476–488. https://doi.org/10.1002/minf.201000061.
Uhr, M., Grauer, M.T., 2003. abcb1ab P-glycoprotein is involved in the uptake of citalopram and trimipramine into the brain of mice. J. Psychiatr. Res. 37, 179–185. https://doi.org/10.1016/S0022-3956(03)00022-0.
Umetrics, A.B., 2008. SIMCA P+ Program, Version, 12.0.0.0. Umea, Sweden.
Vanommeslaeghe, K., Hatcher, E., Acharya, C., Kundu, S., Zhong, S., Shim, J., Darian, E., Guvench, O., Lopes, P., Vorobyov, I., Mackerell, A.D., 2009. CHARMM general force field: a force field for drug-like molecules compatible with the CHARMM all-atom additive biological force fields. J. Comput. Chem. NA-NA. https://doi.org/10.1002/jcc.21367.
Vucicevic, J., Nikolic, K., Dobričić, V., Agbaba, D., 2015. Prediction of blood–brain barrier permeation of α-adrenergic and imidazoline receptor ligands using PAMPA technique and quantitative-structure permeability relationship analysis. Eur. J. Pharm. Sci. 68, 94–105. https://doi.org/10.1016/j.ejps.2014.12.014.
Wang, J.-S., Taylor, R., Ruan, Y., Donovan, J.L., Markowitz, J.S., Lindsay De Vane, C., 2004. Olanzapine Penetration into Brain is Greater in Transgenic Abcb1a P-glycoprotein-Deficient Mice than FVB1 (Wild-Type) Animals. Neuropsychopharmacology 29, 551–557. https://doi.org/10.1038/sj.npp.1300372.
Wiberg, K.B., 1986. Ab Initio Molecular Orbital Theory by W. J. Hehre, L. Radom, P. v. R. Schleyer, and J. A. Pople, John Wiley, New York, 548pp. Price: $79.95, 1986 J. Comput. Chem. 7, 379. https://doi.org/10.1002/jcc.540070314, 379.
Yoon, C.H., Kim, S.J., Shin, B.S., Lee, K.C., Yoo, S.D., 2006. Rapid Screening of Blood-Brain Barrier Penetration of Drugs Using the Immobilized Artificial Membrane Phosphatidylcholine Column Chromatography. J. Biomol. Screen. 11, 13–20. https://doi.org/10.1177/1087057105281656.
Yu, W., He, X., Vanommeslaeghe, K., MacKerell, A.D., 2012. Extension of the CHARMM general force field to sulfonyl-containing compounds and its utility in biomolecular simulations. J. Comput. Chem. 33, 2451–2468. https://doi.org/10.1002/jcc.23067.
Zhang, L., Zhu, H., Oprea, T.I., Golbraikh, A., Tropsha, A., 2008. QSAR Modeling of the Blood–Brain Barrier Permeability for Diverse Organic Compounds. Pharm. Res. 25, 1902–1914. https://doi.org/10.1007/s11095-008-9609-0.